

ANALYSIS OF NON-LINEAR TRANSMISSION LINES BY FREQUENCY DOMAIN PERTURBATION METHOD

AKIO USHIDA, YUICHI TANJI AND YOSHIFUMI NISHIO

Department of Electrical and Electronic Engineering, Faculty of Engineering, Tokushima University, Tokushima 770, Japan

SUMMARY

We discuss a numerical method for solving *non-linear transmission lines* in the frequency domain. Such transmission lines are widely used for communications such as in GaAs integrated circuits and varactor diode circuits. The circuit equations are described by non-linear partial differential equations, so their analysis is very complicated compared with that of linear transmission lines.

In this paper we propose a *frequency-domain perturbation method* for weakly non-linear transmission lines where the wave-forms are approximated by Fourier expansions and each frequency component is calculated by a modified perturbation method. To improve convergence, we introduce two *new* techniques, the *compensation method* and the *homotopy method*, which help to make the iteration stable and can be applied to a wide class of non-linear transmission lines. We have analysed shock wave phenomena in example. © 1997 by John Wiley & Sons, Ltd. Int. J. Circ. Theor. Appl., vol. 25, 95–105 (1997)

(No. of Figures: 6; No. of Tables: 0; No. of Refs: 20.)

1. INTRODUCTION

Recently the analysis and design of high-speed non-linear systems have become more important in the fields of communications and LSI chips. On the other hand, fast-rise-time electrical devices are crucial for high-speed digital and analogue applications and for wide-bandwidth electronic systems. In GaAs non-linear transmission lines,¹ varactor diode circuits and superconducting transmission lines² the capacitors have non-linear voltage–charge characteristics. The velocity of a travelling wave in these non-linear transmission lines is given by a function of amplitudes as follows:

$$\frac{dx}{dt} = \frac{1}{\sqrt{L(i)C(v)}}$$

If the capacitor and/or inductor are decreasing functions of voltages and currents, the velocity will increase with their amplitudes. Therefore it has an interesting property that the higher part of the wave-form is faster than the lower part of it. This property is applied to many purposes such as picosecond pulse compression, broadband phase modulation,¹ picosecond shock wave generation,^{3,4} MESFET gate mixers⁵ and so on. Since it is not very easy to analyse non-linear transmission lines, some papers discuss the phenomena from the physical point of view.^{1–3,6–8}

On the other hand, the harmonic balance method is known as a powerful method for solving non-linear circuits when the wave-form does not contain many higher harmonics. In Reference 9, shock waves in non-linear transmission lines are analysed by the harmonic balance method, where the line is approximated by a finite number of discrete lumped models driven by a sinusoidal wave generator. Note that the harmonic balance method can be efficiently applied only when the number of discrete models is not too large. The shock wave is one of the important phenomena in non-linear transmission lines. In Reference 10 it has been analysed by applying the *difference approximation* to the non-linear partial differential equations. In Reference 11, non-linear wave propagation phenomena are analysed by two-dimensional FFT. On the other hand, device models of IC chips are also described by non-linear partial differential equations^{12,13} and estimation of the

delay time bound is also an important problem in the design of IC chips. In Reference 12 it is calculated using the *RC* discrete model.

In this paper we discuss an efficient numerical method for solving non-linear transmission lines. We approximate the wave-form by a Fourier expansion at each point on the line and the coefficients are calculated by a perturbation technique. Although the perturbation method is only applicable to weakly non-linear systems, we have improved the property by introducing two techniques. The first one reduces the perturbed term by introducing a *negative compensation component*. The second one gradually increases the perturbed term step-by-step from zero to a specified value, which is the same technique as the *homotopy method*.¹⁴ The ideas will be applicable to the analysis of wide classes of non-linear circuits.

In Section 3 we apply our method to the analysis of shock waves in non-linear transmission lines. We find from the example that the convergence ratio is greatly improved by the introduction of the compensation and homotopy methods.

2. FREQUENCY DOMAIN PERTURBATION METHOD

2.1. Perturbation method applied to non-linear transmission lines

There are many kinds of non-linear elements such as Schottky barrier, metal-insulator-semiconductor (MIS) and GaAs integrated transmission lines^{1-4,9} which are used for harmonic and shock wave generation at microwave lengths. Their structures can be approximately described by a discrete model per small length (dx) in the spatial co-ordinate as shown in Figure 1. Thus the circuit is described by the non-linear partial differential equations

$$-\frac{\partial v}{\partial x} = \frac{\partial \phi_L}{\partial t} + v_R, \quad -\frac{\partial i}{\partial x} = \frac{\partial q_C}{\partial t} + i_G \quad (1)$$

where ϕ_L and q_C are the flux of the non-linear inductor and the charge of the non-linear capacitor respectively. We assume the non-linear characteristics

$$i_L = \Gamma \phi_L + \varepsilon \hat{i}_L(\phi_L), \quad v_R = R i_R + \varepsilon \hat{v}_R(i_R) \quad (2a)$$

$$v_C = S q_C + \varepsilon \hat{v}_C(q_C), \quad i_G = G v_G + \varepsilon \hat{i}_G(v_G) \quad (2b)$$

where ε is a small constant and $\hat{i}_L(\phi_L)$, $\hat{v}_R(i_R)$, $\hat{v}_C(q_C)$ and $\hat{i}_G(v_G)$ are non-linear terms. From the circuit model in Figure 1, we have the relations $i \equiv i_L = i_R$ and $v \equiv v_C = v_G$.

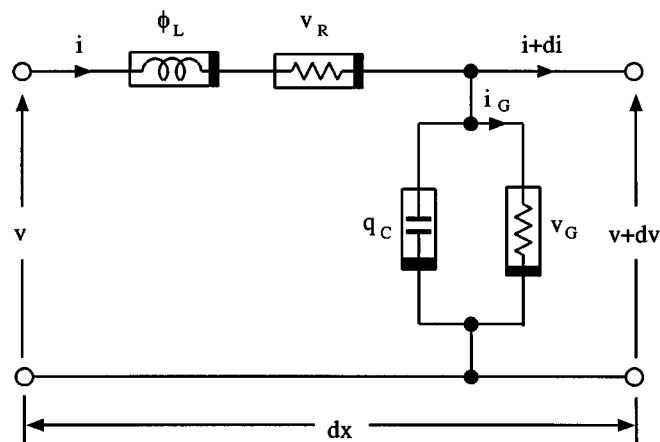


Fig. 1. Discrete model of non-linear transmission line

To analyse shock waves, consider the input impulse wave-form

$$e(t) = \begin{cases} E_m \sin[(2k\pi/T)t], & 0 \leq t \leq T/2k \\ 0, & T/2k \leq t \leq T \end{cases} \quad (3)$$

where T is the period of the impulse and k is an integer. An example of this wave-form is shown in Figure 5 where $T = 1$ ns, $E_m = 0.25$ V and $k = 16$ (see Section 3).

In order to apply the *frequency domain* approach, we describe it by a Fourier expansion in the complex domain as

$$e(t) = \sum_{k=-M}^M E_k e^{jk\omega t}, \quad \omega = 2\pi/T \quad (4)$$

for sufficiently large M . Let us describe the steady-state responses in Fourier expansions as

$$v(x, t) = \sum_{k=-M}^M V_k(x) e^{jk\omega t}, \quad i(x, t) = \sum_{k=-M}^M I_k(x) e^{jk\omega t} \quad (5a)$$

$$\phi_L(x, t) = \sum_{k=-M}^M \Phi_k(x) e^{jk\omega t}, \quad q_C(x, t) = \sum_{k=-M}^M Q_k(x) e^{jk\omega t} \quad (5b)$$

Substituting (5) into (1) and (2), we get the relations

$$-\frac{dV_k}{dx} = jk\omega\Phi_k + RI_k + \varepsilon\hat{V}_{R,k}(i) \quad (6a)$$

$$-\frac{dI_k}{dx} = jk\omega Q_k + GV_k + \varepsilon\hat{I}_{G,k}(v) \quad (6b)$$

$$I_k = \Gamma\Phi_k + \varepsilon\hat{I}_{L,k}(\phi_L) \quad (6c)$$

$$V_k = SQ_k + \varepsilon\hat{V}_{C,k}(q_C) \quad (6d)$$

where $\varepsilon\hat{V}_{R,k}(i)$, $\varepsilon\hat{I}_{G,k}(v)$, $\varepsilon\hat{I}_{L,k}(\phi_L)$ and $\varepsilon\hat{V}_{C,k}(q_C)$ are the k th frequency components obtained from the non-linear terms. Observe that since the non-linear terms are functions of $2M + 1$ Fourier coefficients, the solutions of (6) satisfying the terminal relations are calculated by solving the non-linear two-point boundary value problem in $4(2M + 1)$ dimensions.¹⁵ This is really time-consuming when the frequency components are increased. Fortunately, if the non-linear terms are small enough compared with the linear terms, the *perturbation method*¹⁶ can be efficiently applied to solve (6).

Now let us assume the solutions at the m th iteration as

$$v^m(x, t) = \sum_{k=-M}^M V_k^m(x) e^{jk\omega t}, \quad i^m(x, t) = \sum_{k=-M}^M I_k^m(x) e^{jk\omega t} \quad (7a)$$

$$\phi_L^m(x, t) = \sum_{k=-M}^M \Phi_k^m(x) e^{jk\omega t}, \quad q_C^m(x, t) = \sum_{k=-M}^M Q_k^m(x) e^{jk\omega t} \quad (7b)$$

Then from (6) and (7) the perturbed equations are written in the forms

$$\frac{dV_k^m}{dx} = -(R + jk\omega L)I_k^m - \varepsilon [\hat{V}_{R,k}(i^{m-1}) - jk\omega L\hat{I}_{L,k}(\phi_L^{m-1})] \quad (8a)$$

$$\frac{dI_k^m}{dx} = -(G + jk\omega C)V_k^m - \varepsilon [\hat{I}_{G,k}(v^{m-1}) - jk\omega C\hat{V}_{C,k}(q_C^{m-1})] \quad (8b)$$

where $L = 1/\Gamma$, $C = 1/S$ and

$$\Phi_k^m = L [I_k^m - \varepsilon\hat{I}_{L,k}(\phi_L^{m-1})] \quad (8c)$$

$$Q_k^m = C [V_k^m - \varepsilon\hat{V}_{C,k}(q_C^{m-1})] \quad (8d)$$

Observe that relations (8a) and (8b) are ordinary differential equations w.r.t. the distance x whose second terms on the right-hand side correspond to the forced terms obtained at the $(m - 1)$ th iteration. Φ_k^m and Q_k^m can be decided from (8c) and (8d) after solving (8a) and (8b).

The solutions of (8a) and (8b) are written as

$$V_k^m(x) = A_k^m e^{\lambda_k x} + B_k^m e^{-\lambda_k x} + \varepsilon \hat{V}_k^m(x) \quad (9a)$$

$$I_k^m(x) = \frac{1}{Z_{k,0}} (-A_k^m e^{\lambda_k x} + B_k^m e^{-\lambda_k x}) + \varepsilon \hat{I}_k^m(x) \quad (9b)$$

where the propagation constant λ_k and characteristic impedance $Z_{k,0}$ for the k th frequency component are given by

$$\lambda_k = \sqrt{[(jk\omega L + R)(jk\omega C + G)]}, \quad Z_{k,0} = \sqrt{\left(\frac{jk\omega L + R}{jk\omega C + G}\right)}$$

The first two terms of (9) correspond to the *zero-input responses*; $\varepsilon \hat{V}_k^m(x)$ and $\varepsilon \hat{I}_k^m(x)$ are the *zero-state responses*,¹⁷ which can be calculated by a numerical intergration technique such as backward difference.¹⁸ Here the constant parameters A_k and B_k in (9) are evaluated by the boundary conditions of the transmission line. When it is terminated by the impedance Z_L at the far end, they are given as

$$A_k^m = \frac{\varepsilon \left[\hat{I}_k^m(l) Z_L(jk\omega) - \hat{V}_k^m(l) \right] Z_{k,0} - [Z_{k,0} - Z_L(jk\omega)] E_k e^{-\lambda_k l}}{[Z_{k,0} + Z_L(jk\omega)] e^{\lambda_k l} - [Z_{k,0} - Z_L(jk\omega)] e^{-\lambda_k l}} \quad (10a)$$

$$B_k^m = \frac{\varepsilon \left[-\hat{I}_k^m(l) Z_L(jk\omega) + \hat{V}_k^m(l) \right] Z_{k,0} + [Z_{k,0} + Z_L(jk\omega)] E_k e^{\lambda_k l}}{[Z_{k,0} + Z_L(jk\omega)] e^{\lambda_k l} - [Z_{k,0} - Z_L(jk\omega)] e^{-\lambda_k l}} \quad (10b)$$

Thus the steady state wave-forms at the m th iteration are estimated by (5a) and (5b).

The iteration will be continued until the variation

$$\delta_m \equiv \sqrt{\left(\sum_{k=-M}^M [V_k^m(l) - V_k^{m-1}(l)]^2 + \sum_{k=-M}^M [I_k^m(l) - I_k^{m-1}(l)]^2 \right)} \quad (11)$$

becomes sufficiently small for a given constant δ . Note that we cannot say whether the solution wave-form is sufficiently accurate or not. Thus let us define the following *residual error*. Assume that the solutions for M frequency components are $v_M(l, t)$ and $i_M(l, t)$ and that the exact solutions are $\hat{v}(l, t)$ and $\hat{i}(l, t)$. Then the *residual error* is defined as

$$\varepsilon_M \equiv \sqrt{\left(\frac{1}{T} \int_0^T \{ [v_M(l, t) - \hat{v}(l, t)]^2 + [i_M(l, t) - \hat{i}(l, t)]^2 \} dt \right)} \quad (12)$$

Since it is impossible to get the exact solutions, we assume $v_{M'}(x, t)$ and $i_{M'}(x, t)$ as the exact solutions which are obtained with a larger number of frequency components ($M' \gg M$). Then we have

$$\varepsilon_M \approx \sqrt{\left(\sum_{|k|=M}^{M'} [V_k^M(l) - V_k^{M'}(l)]^2 + \sum_{|k|=M}^{M'} [I_k^M(l) - I_k^{M'}(l)]^2 \right)}$$

If the residual error ε_M is not small enough, we need to choose a much larger M for the approximation and again try our perturbation method.

2.2. Improvements in perturbation method

It is known that the perturbation method¹⁶ can be applied only to weakly non-linear circuits. In this subsection we improve the method such that it can be applied to a wider class of non-linear circuits.

Assume that the non-linear characteristics given in (2) are monotone increasing functions. For simplicity we describe the situation as

$$u_1 = H u_2 + \varepsilon \hat{h}(u_2) \quad (13)$$

where $u_1 = (i_L, v_R, v_C, i_G)^T$, $u_2 = (\phi_L, i_R, q_C, v_G)^T$ and

$$H = \text{diag}(\Gamma, R, S, G), \quad \varepsilon \hat{h}(u_2) = \varepsilon (\hat{i}_L(\phi_L), \hat{v}_R(i_R), \hat{v}_C(q_C), \hat{i}_G(v_G))^T$$

To improve the convergence ratio of our perturbation method, we try to reduce the perturbed term $\varepsilon \hat{h}(u_2)$. Let us introduce a small constant

$$\Delta H \equiv \text{diag}(\Delta \Gamma, \Delta R, \Delta S, \Delta G)$$

as the *compensation parameter* in the form

$$u_1 = (H + \Delta H)u_2 + [\varepsilon \hat{h}(u_2) - \Delta H u_2] \tag{14}$$

The second term corresponds to the perturbed term, which can be greatly reduced by choosing a suitable ΔH . We found from our numerical example that the convergence ratio is greatly improved even for a small *compensation parameter* ΔH .

The *homotopy method*¹⁴ is sometimes used when the iteration method does not guarantee convergence. It has the property of global convergence. We will apply it to our perturbation method. Let us introduce a parameter ρ for the non-linear elements as follows:

$$u_1 = (H + \Delta H)u_2 + \rho[\varepsilon \hat{h}(u_2) - \Delta H u_2], \quad \rho: 0 \rightarrow 1 \tag{15}$$

It is clear that relation (15) for $\rho = 0$ corresponds to the linear case and that the non-linearity is gradually increased by choosing $\{\rho: 0 \rightarrow 1\}$. At $\rho = 1$ it is reduced to the original equation. If we choose a small variation $\Delta \rho$ per iteration such as

$$\rho^m = \rho^{m-1} + \Delta \rho$$

our perturbation method can get the solution stably.

2.3. Convergence conditions

Now let us consider the convergence conditions of our perturbation method. For simplicity let us introduce the following notation for the variables in (8) and (9).

(a) For the solutions we set

$$X_{1,k}^m(x) = \begin{pmatrix} V_k^m(x) \\ I_k^m(x) \end{pmatrix}, \quad X_{2,k}^m(x) = \begin{pmatrix} \Phi_k^m(x) \\ Q_k^m(x) \end{pmatrix} \tag{16a}$$

(b) For the perturbed terms we set

$$\hat{X}_{1,k}(w_1^{m-1}, x) = \begin{pmatrix} \hat{V}_{R,k}(i^{m-1}) \\ \hat{I}_{G,k}(v^{m-1}) \end{pmatrix}, \quad \hat{X}_{2,k}(w_2^{m-1}, x) = \begin{pmatrix} \hat{I}_{L,k}(\phi_L^{m-1}) \\ \hat{V}_{C,k}(q_C^{m-1}) \end{pmatrix} \tag{16b}$$

where $w_1 = (v, i)^T$ and $w_2 = (\phi_L, q_C)^T$.

We describe the coefficient matrices of (8) as

$$A_k = \begin{pmatrix} 0 & R + jk\omega L \\ G + jk\omega C & 0 \end{pmatrix}, \quad B_k = \begin{pmatrix} jk\omega L & 0 \\ 0 & jk\omega C \end{pmatrix} \tag{17a}$$

$$C_0 = \begin{pmatrix} 0 & L \\ C & 0 \end{pmatrix} \tag{17b}$$

Now we describe the *zero-state response* of (9) in the integrations. Then we have from (9) and (10)

$$X_{1,k}^m(x) = C_{1,k}(x)E_k + C_{2,k}(x)X_{1,k}^m(l) - \varepsilon \int_0^x e^{-A_k(x-s)} \hat{X}_{1,k}(w_1^{m-1}, s) ds - \varepsilon B_k \int_0^x e^{-A_k(x-s)} \hat{X}_{2,k}(w_2^{m-1}, s) ds \tag{18a}$$

$$X_{2,k}^m(x) = C_0 X_{1,k}^m(x) - \varepsilon C_0 \hat{X}_{2,k}(w_2^{m-1}, x) \tag{18b}$$

where $C_{1,k}(x)$ and $C_{2,k}(x)$ are obtained from (9) and (10).

Let us adopt the norm¹⁹

$$\|w(t)\| \equiv \sqrt{\left(\frac{1}{T} \int_0^T w^2(t) dt\right)} \quad (19)$$

Assume that $w(t)$ is a periodic function of the period T as follows:

$$w(t) = \sum_{k=-M}^M W_k e^{ik\omega t}$$

Then we have the Euclidean norm

$$\|W\| \equiv \sqrt{(|W_{-M}|^2 + |W_{-M+1}|^2 + \dots + |W_M|^2)} \quad (20)$$

Thus the two norms coincide with each other, i.e.

$$\|w(t)\| = \|W\|$$

Now we have the following convergence conditions.

Theorem 1.

Assume that for an approximate solution $(w_1^0, w_2^0)^T$ there are constants D_1, D_2, K_0, L_1 and L_2 satisfying the following:

(i) Define the solution domain by

$$\Omega \equiv \{w_1, w_2 \mid \|w_1 - w_1^0\| \leq D_1, \|w_2 - w_2^0\| \leq D_2\} \quad (21a)$$

(ii) Define the norms of the coefficient matrices by

$$K_0 \equiv \|C_0\|, \quad K_1 \equiv \max_{-M \leq k \leq M} \frac{\|A_k^{-1}\| L_1 l}{1 - C_{2k}}, \quad K_2 \equiv \max_{-M \leq k \leq M} \frac{\|B_k A_k^{-1}\| L_2 l}{1 - C_{2k}} \quad (21b)$$

where

$$C_{2k} \equiv \max_{0 \leq x \leq l} \|C_{2,k}(x)\|$$

(iii) Assume that the perturbed terms satisfy the Lipschitz conditions:

$$\|\hat{X}_1(w_1', x) - \hat{X}_1(w_1'', x)\| \leq L_1 \|w_1' - w_1''\| \quad (21c)$$

$$\|\hat{X}_2(w_2', x) - \hat{X}_2(w_2'', x)\| \leq L_2 \|w_2' - w_2''\| \quad (21d)$$

in Ω for all $0 \leq x \leq l$, where L_1 and L_2 are Lipschitz constants.

(iv) Set the maximum values of the variables in $x = [0, l]$ as

$$X_{1,k}^m = \max_{0 \leq x \leq l} \|X_{1,k}^m(x)\|, \quad X_{2,k}^m = \max_{0 \leq x \leq l} \|X_{2,k}^m(x)\| \quad (21e)$$

Furthermore, if it satisfies the condition

$$\kappa \equiv \varepsilon \|P\| < 1, \quad \text{for } P = \begin{pmatrix} K_1 & K_2 \\ K_0 K_1 & K_0(K_2 + L_2) \end{pmatrix} \quad (22)$$

our perturbation method (18) will converge to the unique solution $(\bar{w}_1, \bar{w}_2)^T$.

Proof. For non-linear transmission lines we can assume $\|e^{-A_k x}\| \leq 1$ for $0 \leq x \leq l$. Hence we have from (18a) and (21b)¹⁷

$$\|X_{1,k}^m(x) - X_{1,k}^{m-1}(x)\| \leq C_{2k} \|X_{1,k}^m(l) - X_{1,k}^{m-1}(l)\|$$

$$\begin{aligned}
 & +\varepsilon \| A_k^{-1} \| \int_0^x \| \hat{X}_{1,k}(w_1^{m-1}, s) - \hat{X}_{1,k}(w_1^{m-2}, s) \| ds \\
 & +\varepsilon \| B_k A_k^{-1} \| \int_0^x \| \hat{X}_{2,k}(w_2^{m-1}, s) - \hat{X}_{2,k}(w_2^{m-2}, s) \| ds
 \end{aligned}$$

Applying the Lipschitz conditions (21c) and (21d), we have

$$\sum_{k=-M}^M \| X_{1,k}^m - X_{1,k}^{m-1} \| \leq \varepsilon K_1 \sum_{k=-M}^M \| X_{1,k}^{m-1} - X_{1,k}^{m-2} \| + \varepsilon K_2 \sum_{k=-M}^M \| X_{2,k}^{m-1} - X_{2,k}^{m-2} \|$$

Thus we have from (20)

$$\| X_1^m - X_1^{m-1} \| \leq \varepsilon K_1 \| X_1^{m-1} - X_1^{m-2} \| + \varepsilon K_2 \| X_2^{m-1} - X_2^{m-2} \| \tag{23a}$$

In the same manner we have from (18b)

$$\| X_2^m - X_2^{m-1} \| \leq K_0 \| X_1^m - X_1^{m-1} \| + \varepsilon K_0 L_2 \| X_2^{m-1} - X_2^{m-2} \| \tag{23b}$$

Set $X = (X_1, X_2)^T$. Then we have from (22) and (23)

$$\| X^m - X^{m-1} \| \leq \kappa \| X^{m-1} - X^{m-2} \| \tag{24}$$

Hence

$$\| X^m - X^{m-1} \| \leq \kappa^{m-1} \| X^1 - X^0 \|$$

Thus our perturbation method will converge to the solution \bar{X} and the error bound of the approximate solution X^0 is estimated as

$$\begin{aligned}
 \| X^m - X^0 \| & \leq \| X^m - X^{m-1} \| + \| X^{m-1} - X^{m-2} \| + \dots + \| X^1 - X^0 \| \\
 & \leq (\kappa^{m-1} + \kappa^{m-2} + \dots + \kappa + 1) \| X^1 - X^0 \| \\
 & = \frac{1 - \kappa^m}{1 - \kappa} \| X^1 - X^0 \|
 \end{aligned}$$

Thus we have proved the convergence condition.

Q.E.D

We found from the Theorem 1 that our perturbation method will converge to an approximate solution \bar{X} if the non-linear term ε is sufficiently small.

3. ILLUSTRATIVE EXAMPLE

As an example of non-linear transmission lines, let us calculate the shock wave due to an impulse. Assume that the line is terminated by a resistor $R_L = 10 \Omega$. For simplicity, we assume that the inductor is linear and the other characteristics in (2) are given as

$$i_L = 350 \times 10^{11} \phi_L, \quad v_R = 0.015 i_R + 0.1 i_R^3, \quad v_C = 10^{11} q_C + 0.5 \times 10^{34} q_C^3, \quad i_G = 0.015 v_G + 0.1 v_G^3$$

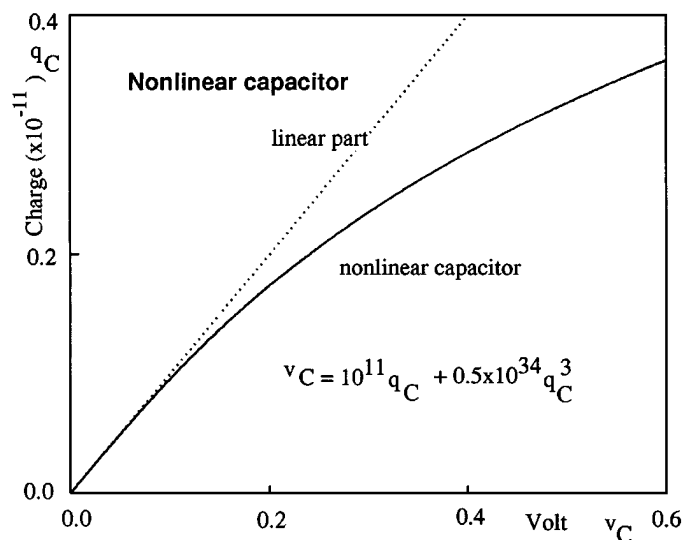


Fig. 2. Characteristic curve of non-linear capacitor: $v_C = 10^{11}q_C + 0.5 \times 10^{34}q_C^3$

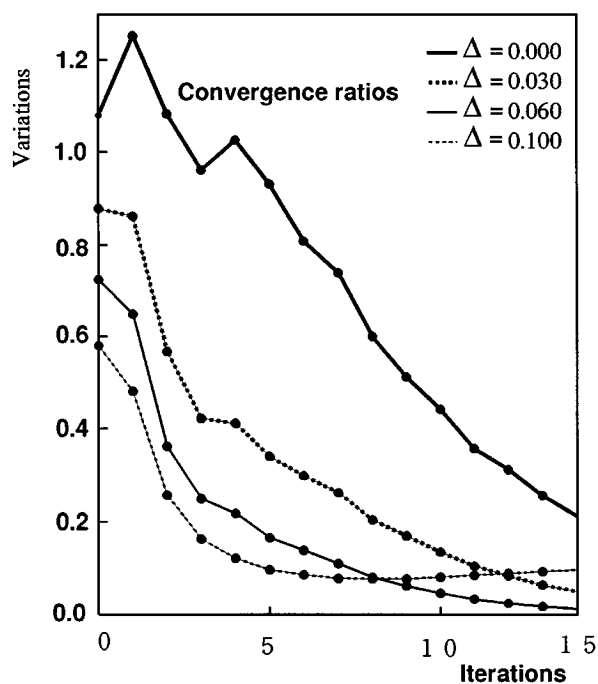


Fig. 3. Convergence ratios for various compensation parameters, where variations are defined by $\delta_m = \|X^m(l) - X^{m-1}(l)\|$

The $q-v$ characteristic curve is shown in Figure 2. We assume $E_m = 0.25 V, T = 1 ns$ and $k = 16$ for the input impulse in (3). For the calculation of zero-state responses in (8) we applied the first- and/or second-order backward difference formulae¹⁸, where the step size is chosen as $\Delta x = l/60$.

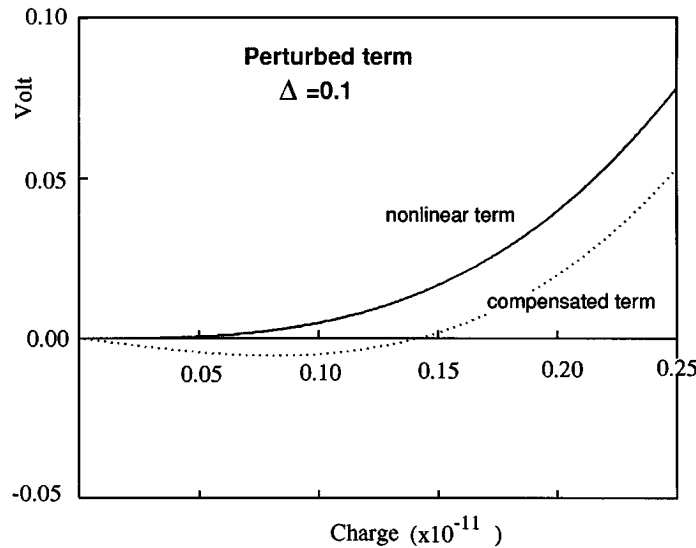


Fig. 4. Perturbed term by compensation method for $\Delta = 0.1$. $\hat{v}_C = 0.5 \times 10^{34} q_C^3 - 0.1 \times 10^{11} q_C$

The convergence ratios are shown in Figure 3 for various compensation parameters ΔH . In this case the variations are estimated by

$$\delta_m = \left\| \left(\sum_{k=-128}^{128} [V_k^m(I) - V_k^{m-1}(I)]^2 + \sum_{k=-128}^{128} [I_k^m(I) - I_k^{m-1}(I)]^2 \right)^{1/2} \right\|$$

We found from the results that the convergence will be greatly improved even for a small Δ in (14). Figure 4 shows the perturbed term for $\Delta = 0.1$:

$$\hat{v}_C = 0.5 \times 10^{34} q_C^3 - 0.1 \times 10^{11} q_C$$

When we applied both the *compensation method* with $\Delta = 0.03$ and the *homotopy method* with

$$\rho^m = \rho^{m-1} + 0.1, \quad \text{for } m \leq 10, \quad \rho = 1 \quad \text{for } m > 10$$

our method could get the solution stably. The wave-forms are shown in Figures 5 and 6, where we assumed 128 frequency components. Wave-form (a) in Figure 5 is the response of the non-linear transmission line, while wave-form (b) shows the linear response neglecting non-linear terms. The features of the shock wave are apparent in the non-linear response. Wave-form (c) is the input impulse wave-form. The residual error defined by (12) for $M' = 256$ is given by

$$\Delta_{128} = 0.97 \times 10^{-2}$$

The error in the amplitude is about 2.4%, which seems to be accurate enough.

We remark that although the perturbation method never converges for the stronger non-linear term

$$v_C = 10^{11} q_C + 0.8 \times 10^{34} q_C^3 \tag{25}$$

with $\Delta = 0$, our perturbation method with $\Delta = 0.1$ can get the solution stably.

Thus we found from the example that our perturbation method is greatly improved by incorporating the two techniques of *compensation* and *homotopy*.

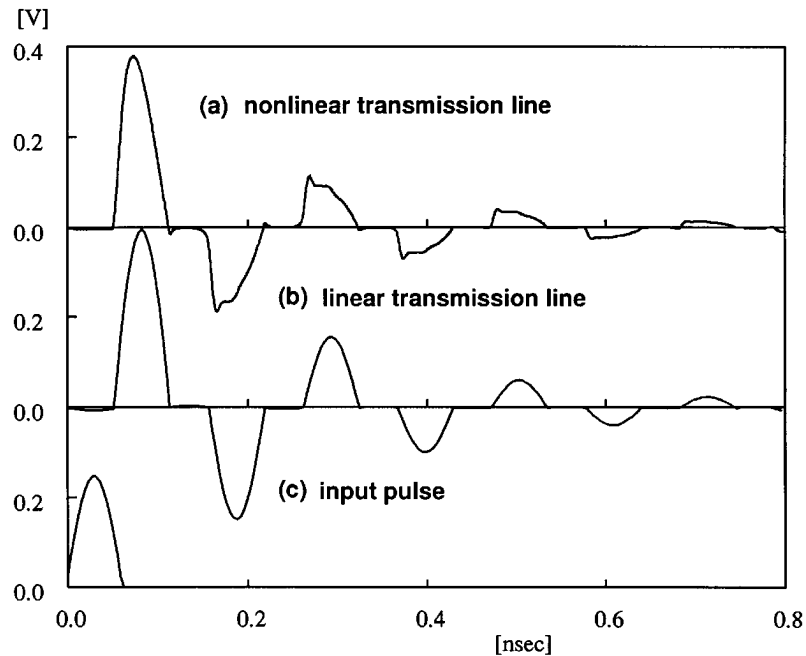


Fig. 5. Impulse responses: (a) response of non-linear transmission line; (b) response of linear transmission line neglecting non-linear terms; (c) input impulse, ($E_m = 0.25$ V, $T = 1$ ns, and $k = 16$ in (3))

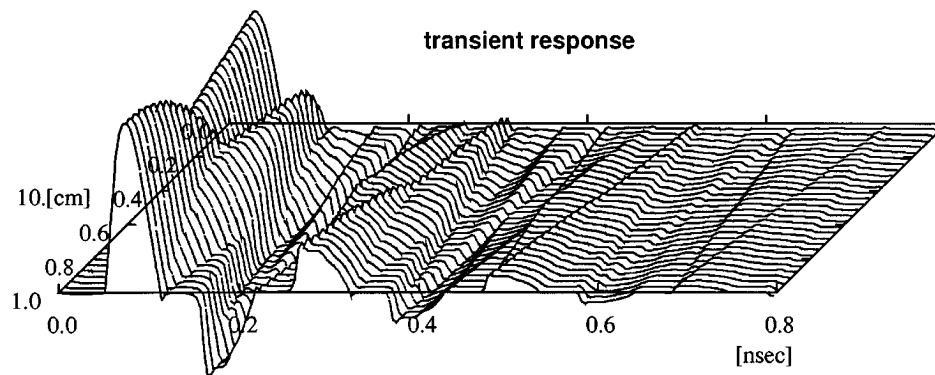


Fig. 6. Response of non-linear transmission line in (x, t) domain ($l = 10$ cm, $T = 1$ ns, $E_m = 0.25$ V, $R_L = 10 \Omega$)

4. CONCLUSIONS AND REMARKS

We have presented a frequency domain perturbation algorithm for calculating transient responses of non-linear transmission lines. We can greatly improve the convergence by introducing two techniques, the *compensation method* and the *homotopy method*. They have the properties of improving the convergence ratios and stabilizing the iteration by reducing the perturbed terms. Thus our perturbation method becomes much more powerful for the analysis of non-linear transmission lines.

Note that since the algorithm in this paper is based on the perturbation method, convergence may not be guaranteed even if we choose any Δ and $\Delta\rho$ for strong non-linearity. The non-linearity of the element depends on the amplitude of the input variable and can be estimated by the ratio (non-linear term)/

(linear term). In the example of (2) we have about 0.5 at $v_C = 0.4$. We found from our numerical experiences that we cannot hope for convergence when the ratio is greater than unity.

Most practical circuits such as GaAs transmission lines¹ belong to the class of non-linear RC transmission lines. They are special cases of our example where our algorithm can be efficiently applied to much stronger non-linearity.

REFERENCES

1. M. J. W. Rodwell, 'Nonlinear transmission line for picosecond pulse compression and broadband phase modulation', *Electron. Lett.*, **23**, 109–110 (1987).
2. R. K. Arora and J. L. Thaker, 'Electromagnetic pulse transmission on superconducting interconnects', *Int. J. Electron.*, **71**, 117–125 (1991).
3. C. J. Madden, R. A. Marsland, M. J. W. Rodwell, D. M. Bloom and Y. C. Pao, 'Hyperabrupt-doped GaAs nonlinear transmission line for picosecond shock wave generation', *Appl. Phys. Lett.*, **54**, 1019–1021 (1989).
4. K. S. Champlin and D. R. Singh, 'Small-signal second-harmonic generation by a non-linear transmission line', *IEEE Trans. Microwave Theory Tech.*, **MTT-34**, 351–353 (1986).
5. C. Camacho-Penalosa and C. S. Aitchison, 'Analysis and design of MESFET gate mixers', *IEEE Trans. Microwave Theory Tech.*, **MTT-35**, 643–652 (1987).
6. F. A. Benson and J. D. Last, 'Non-linear-transmission-line harmonic generator', *Proc. IEE*, **112**, 635–643 (1965).
7. R. Landauer, 'Shock waves in nonlinear transmission lines and their effect on parametric amplification', *IBM J.*, October, pp. 391–401 (1960).
8. D. Jager and F. -J. Tegude, 'Non-linear wave propagation along periodic-loaded transmission line', *Appl. Phys.*, **15**, 393–397 (1978).
9. C. Camacho-Penalosa and I. Molina-Fernandez, 'Harmonic balance analysis of non-linear transmission lines', *Electron. Lett.*, **24**, 1235–1236 (1988).
10. R. H. Freeman and A. E. Karbowiak, 'An investigation of nonlinear transmission lines and shock waves', *J. Phys. D: Appl. Phys.*, **10**, 633–643 (1977).
11. I. Molina-Fernandez, C. Camacho-Penalosa and J. Ramos, 'Application of the two-dimensional Fourier transform to non linear wave propagation phenomena', *IEEE Trans. Microwave Theory Tech.*, **42**, 1079–1085 (1994).
12. C. A. Marinov and P. Peittaanmaki, 'A delay time bound for distributed parameter circuits with bipolar transistors', *Int. j. cir. theor. appl.*, **18**, 99–106 (1990).
13. J. L. Wyatt Jr., 'Monoton sensitivity of nonlinear nonuniform RC transmission lines with application to timing analysis of digital MOS integrated circuits', *IEEE Trans. Circuits and Systems*, **CAS-32**, 28–83 (1985).
14. C. B. Garcia and W. I. Zangwill, *Pathways to Solutions, Fixed Points, and Equilibria*, Prentice-Hall, Englewood Cliffs, NJ, 1981.
15. S. M. Roberts and J. S. Shipman, *Two-Point Boundary Value Problems: Shooting Methods*, American Elsevier, New York, 1972.
16. J. Kevorkian and J. D. Cole, *Perturbation Methods in Applied Mathematics*, Springer, New York, 1981.
17. L. A. Zadeh and C. A. Desoer, *Linear System Theory: the State Space Approach*, McGraw-Hill, New York, 1963.
18. L. O. Chua and P.-M. Lin, *Computer-Aided Analysis of Electrical Circuits: Algorithms and Computational Techniques*, Prentice-Hall, Englewood Cliffs, NJ, 1975.
19. M. Urabe, 'Galerkin's procedure for nonlinear periodic systems', *Arch. Rat. Mech. Anal.*, **20**, 120–152 (1965).
20. A. Ushida, T. Adachi and L. O. Chua, 'Steady-state analysis of non-linear circuits based on hybrid method', *IEEE Trans. Circuits and Systems—I*, **CAS 39**, 649–661 (1992).